JP Journal of Heat and Mass Transfer

http://www.pphmj.com
http://dx.doi.org/10.17654/HM014020227
Volume 14, Number 2, 2017, Pages 227-246 **ISSN: 0973-5763**

RADIATIVE ENTROPY GENERATION DUE TO EQUI-DISTRIBUTION OF INCIDENT ANISOTROPIC RADIATION THROUGH A DIFFUSE REFLECTION

A. Mazgar[1,2,*], A. Sakly[1], F. Hajji[1] and F. Ben Nejma[1]

[1]The Unit of Ionized and Reactive Media Study
Preparatory Institute for Engineering Studies of Monastir
Ibn Eljazzar Street, 5019 Monastir, Tunisia

[2]The Institute of Applied Sciences and Technology of Mahdia
Sidi Massoud, 5100 Mahdia, Tunisia

Abstract

In this work, we analyze through a numerical study, the radiative entropy generation at a perfectly reflecting and diffuse wall. The study is a valuable experience because it studies first the behaviour of thermal radiation within a diffuse wall for two different geometries and second, it evaluates entropy creation due to radiation in an adiabatic surface. The effect scales of key parameters on wall radiative entropy production are determined. It is noticed that entropy generated through the perfectly reflecting and diffuse wall is far from being negligible, even if thermal exchanges are absent.

Received: March 24, 2016; Revised: June 3, 2016; Accepted: June 25, 2016

Keywords and phrases: entropy, anisotropy, thermal radiation, diffuse reflection, equi-distribution.

*Corresponding author

Communicated by Zekeriya Altac

Nomenclature

c : speed of light in vacuum $(\mathrm{m} \cdot \mathrm{s}^{-1})$

f : aspect ratio, $f = \dfrac{L_y}{L_x}$

F_d : view factor

H : width of the plates (m)

h : Plank's constant $(h = 6.626 \times 10^{-34}\,\mathrm{J} \cdot \mathrm{s})$

I : radiation intensity $(\mathrm{W} \cdot \mathrm{m}^{-2} \cdot \mathrm{sr}^{-1})$

k_B : Boltzmann's constant $(k_B = 1.38 \times 10^{-23}\,\mathrm{J} \cdot \mathrm{K}^{-1})$

K : absorption coefficient

Lx : channel length (m)

Ly : channel width (m)

q_{ri} : incident radiative flux (kWm^{-2})

S : wall entropy $(\mathrm{W} \cdot \mathrm{K} \cdot \mathrm{m}^{-2})$

S_g : wall entropy generation $(\mathrm{W} \cdot \mathrm{K} \cdot \mathrm{m}^{-2})$

T : temperature (K)

x, y : Cartesian coordinates

Greek symbols

ν : frequency (s^{-1})

$\breve{\nu}$: wavenumber (cm^{-1})

$\vec{\Omega}$: ray direction

$d\Omega$: elementary solid angle around $\vec{\Omega}$

σ : Stefan-Boltzmann constant $(\sigma = 5.670 \times 10^{-8}\,\mathrm{W \cdot m^{-2} \cdot K^{-4}})$

ε : wall emissivity

Superscript

b : black body

Subscripts

a : ambient

w : wall

v : spectral

0 : bottom wall

1 : upper wall

2 : lateral walls

Introduction

The analysis of the energy utilization and the entropy generation becomes one of the primary objectives in designing thermal systems. That is to say, the analysis of entropy production or thermodynamic irreversibility is shared to all heat transfer types such as turbo machinery, heat exchangers and electronic cooling. Moreover, the analysis of the second law allows minimizing entropy production to higher energy efficiency. Bejan [2, 3] introduces the notion of irreversibility distribution ratio and entropy generation number, exhibiting spatial distribution profiles of entropy generation. As a matter of fact, he proposes different analytical expressions for both entropy production in a circular duct and for several engineering processes. San et al. [20, 21] use the analogy between heat and mass transfer in order to determine entropy generation for optimum plate spacing and Reynolds number.

Thermal radiation is encountered in a wide range of thermal engineering applications like furnaces, boilers, solar collectors and other combustion systems. For instance, we can cite, in particular, the solar concentrators which represent a device that permits the collection of sunlight from a large area and focusing it on a smaller receiver or exit. For such industrial application, the sunlight is concentrated in order to exploit thermal energy through a diffuse and isotropic reflection. By contrast, the evaluation of entropy production owing to radiative heat transfer in a semi-transparent medium has often been neglected. Based on the interaction of monochromatic radiation with a system of independent ideal oscillators, Planck [19] shows that the sum of the entropy changes of the radiative field and the system of oscillators is always positive or zero. He is among the first to present researches dealing with entropy generation through radiative transfer as he studies the interaction of light and matter with respect to its irreversibility [18]. Moreover, Wildt [22] formulates the transfer equation for radiative entropy by analyzing the steady-state interaction of the non-isotropic field of non-equilibrium radiation with an isotropic atom gas. In addition, Oxenius [17] analyzes some properties of the radiative entropy generation through an isothermal atmosphere and proves that the total local entropy which is created in this atmosphere is not negative. Kröll [11] studies the properties of entropy generation due to radiative heat transfer by analyzing its general form and its sign. He demonstrates that corresponding equation can be written in a bilinear form. Wright et al. [23] present a numerical investigation to simplify the calculation of radiative entropy creation for grey and non-participating media, considering the entropy components associated with absorption, emission, and reflection of radiation. Following the approach of Planck's theory for radiative entropy, Caldas and Semiao [7] derive the radiative entropy transfer equation in semi-transparent media and present a numerical method to compute the corresponding radiative entropy production. They deduce that entropy generated through scattering is less than that produced through emission and absorption. Caldas and Semiao [8] investigate the effects of turbulence-radiation interaction on entropy generation. They show that both entropy generation and heat transfer

are approximately proportional to the square of the intensity of turbulence. Liu and Chu [12] diagnose the classical formula of entropy creation rate for heat transfer, to conclude that it cannot be used to calculate the local entropy generation rate of radiative heat transfer. In tandem with this work, Liu and Chu [14] extend the numerical simulation of Caldas and Semiao [7] about radiative entropy generation through participating media, to analyze the radiative entropy creation in the enclosures filled with semi-transparent media. Liu and Chu [13] give the radiative exergy transfer equation and verify its consistency with the Gouy-Stodola theorem in classical thermodynamics. Agudelo and Cortés [1] present a review of publications about second law analysis and thermal radiation, including exchange between surfaces, the presence of a participative medium and the analysis of combined heat transfers. Wu and Liu [24] submit a critical review of entropy creation flux due to radiative heat transfer, giving a special attention to Earth's radiation entropy flux and revealing that the important difference in the Earth's reflected solar radiation entropy flux between the different expressions arises principally from the difference of the Earth's reflection properties. Kabelac and Conrad [10] perform numerical analyses of entropy calculations for radiation fluxes applied to simple radiation-surface interactions, preparing the way towards an entropy generation minimization analysis of more complex radiation settings. The second law of thermodynamics corresponding to the radiative transfer between two isothermal surfaces is analyzed by Zhang and Basu [25] giving evaluation of entropy flux and generation in radiative heat transfer for non-ideal surfaces. Ben Nejma et al. [4] study entropy generation through combined non-grey gas radiation and forced convection between parallel plates. They examine the radiative contribution in the volumetric entropy generation. Mazgar et al. [15] extend the preceding study to evaluate entropy creation through combined non-grey gas radiation and natural convection in a vertical pipe. Ben Nejma et al. [5, 6] propose numerical analyses of radiative entropy creation through non-grey media confined in spherical and cylindrical enclosures, respectively. Mazgar et al. [16] numerically investigate second law analysis of coupled mixed convection and non-grey gas radiation within

a cylindrical annulus. They conclude that the volumetric entropy generation due to thermal radiation is remarkably developed compared to wall radiative entropy production and to that created due to friction and conduction.

The entropy creation due to the radiative contribution has not been sufficiently studied, especially through anisotropic radiation. The objective of the present work is to highlight entropy production at a perfectly reflecting and diffuse wall through the equi-distribution of an incident anisotropic radiation.

General Formulation

The information contained in this paper deals with a numerical study of radiative entropy production at a totally reflecting wall for parallel plates and a rectangular cavity. In both cases, the diffuse surface receives the incident anisotropic radiation and redistributes it through an isotropic reflected one. The principal idea is to choose an extremely case with a perfectly reflective wall to favour entropy generation due to distribution to the detriment of that produced by thermal exchanges:

$$\Delta S = S_{exchanges} + S_{creation} = S_{creation} > 0. \quad (1)$$

Parallel plates

As can be seen in Figure 1, the physical system consists in an emitting and absorbing semi-transparent medium maintained between two parallel plates. The first wall is assumed as a black surface maintained at a temperature T_w while the second one is totally reflecting.

The incident intensity at the reflecting wall is a function of the incidence angle with regard to the normal of this surface and it is given as follows:

$$I_\nu(\vec{\Omega}) = I_\nu^b(T_w)\exp^{-Kh/\xi(\vec{\Omega})} + I_\nu^b(T_a)(1 - \exp^{-Kh/\xi(\vec{\Omega})}), \quad (2)$$

where $I_\nu^b(\vec{\Omega})$ is the black body spectral radiation energy per unit of solid angle and frequency, as defined by the Planck's law [19]:

$$I_{\nu}^{b}(\vec{\Omega}) = \frac{2h\nu^3}{c^2}\frac{1}{e^{\frac{h\nu}{k_B T}} - 1}. \tag{3}$$

The incident radiation depends on the direction of the radiative propagation and its value is function of the directional radiative temperature to each spectral intensity $I_{\nu}(\vec{\Omega})$, given by:

$$T_{\nu}(\vec{\Omega}) = \frac{dI_{\nu}(\vec{\Omega})}{dS_{\nu}(\vec{\Omega})} = \frac{h\nu}{k_B Ln\left(1 + \frac{2h\nu^3}{c^2 I_{\nu}(\vec{\Omega})}\right)}. \tag{4}$$

The entropy intensity of radiation derived from the spectral radiative intensity is defined by Planck [18] as follows:

$$S_{\nu}(\vec{\Omega}) = \frac{2k_B\nu^2}{c^2}\left[\left(1 + \frac{c^2 I_{\nu}(\vec{\Omega})}{2h\nu^3}\right)Ln\left(1 + \frac{c^2 I_{\nu}(\vec{\Omega})}{2h\nu^3}\right) - \frac{c^2 I_{\nu}(\vec{\Omega})}{2h\nu^3}Ln\left(\frac{c^2 I_{\nu}(\vec{\Omega})}{2h\nu^3}\right)\right]. \tag{5}$$

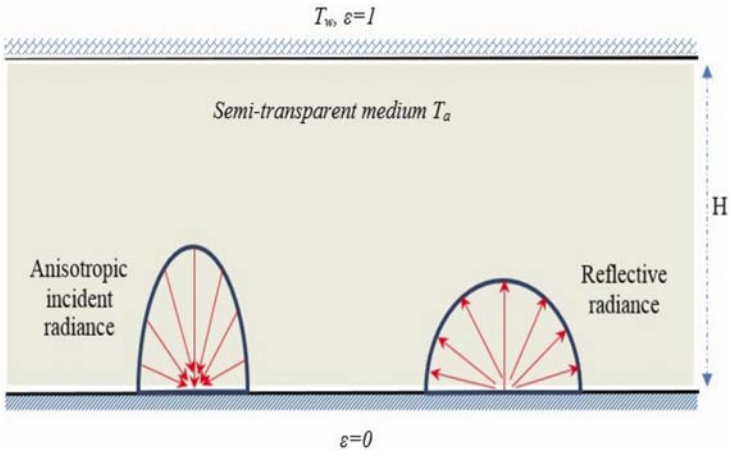

Figure 1. Parallel plates geometry and boundary conditions.

In Figure 2, we draw the curve of the spectral radiation temperature versus incidence angle, indicating the temperature value which is perceived by the reflected radiation coming from the black surface and passing through

the semi-transparent media. As has been noted, the radiative temperature strongly depends upon the spectral position, offering a temperature range between the black surface temperature and the semi-transparent medium one. This temperature is close to the black body temperature for incidence angles close to zero (optically thin medium) and tends toward the confined medium temperature for very oblique incidence angles (optically thick medium).

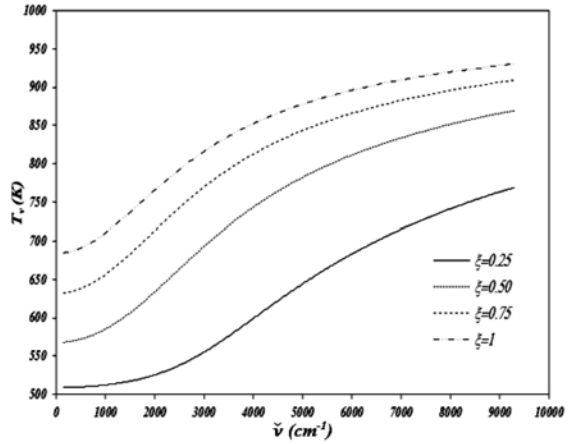

Figure 2. Profiles of the spectral radiation temperature $T_w = 1000\text{K}$, $T_a = 500$ and $K.H = 1$.

The reflected radiation intensity is uniform in all directions and is also defined by:

$$I_{\nu\_ref}(\vec{\Omega}') = \frac{1}{\pi}\int_{\vec{\Omega}\vec{n}<0} I_\nu(\vec{\Omega})\xi(\vec{\Omega})d\vec{\Omega}(\vec{\Omega}'). \tag{6}$$

The hemispheric, total and radiative entropy creation at the perfectly reflecting surface is defined as follows [14]:

$$S_g = \int_{\nu=0}^{\nu=\infty}\int_{4\pi}\left[S_\nu(I_\nu(\vec{\Omega})) - \frac{I_\nu(\vec{\Omega})}{T_w}\right]\xi(\vec{\Omega})d\Omega d\nu. \tag{7}$$

Given the fact that the second plate is considered as a perfectly reflecting wall, equation (7) given above becomes:

$$S_g = \int_{\nu=0}^{\nu=\infty}\int_{4\pi} S_\nu(I_\nu(\vec{\Omega}))\xi(\vec{\Omega})d\Omega d\nu. \tag{8}$$

Rectangular cavity

As shown in Figure 3, the second physical problem under study in this work deals with a non-participating medium confined in a rectangular cavity which is composed of three black surfaces maintained at uniform temperature and a bottom wall supposed to be perfectly reflective. The two horizontal walls are maintained at different temperatures where the lateral ones are held at the same temperature.

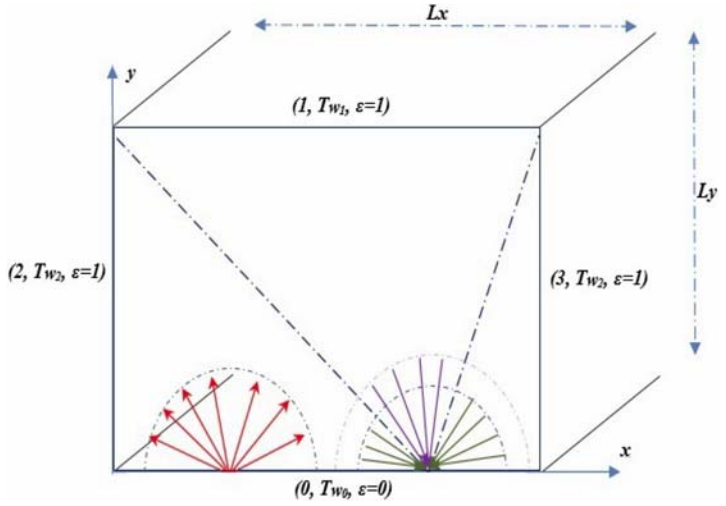

Figure 3. Rectangular cavity geometry and boundary conditions.

The analytical expressions of the various view factors corresponding to the reflecting wall watching the other surfaces are presented by the following equation system:

$$\begin{cases} F_{d(0)\to(1)}(x) = \dfrac{1}{2}\left(\dfrac{x}{\sqrt{L_y^2 + x^2}} + \dfrac{L_x - x}{\sqrt{L_y^2 + (L_x - x)^2}} \right), \\ F_{d(0)\to(2)}(x) = \dfrac{1}{2}\left(1 - \dfrac{x}{\sqrt{L_y^2 + x^2}} \right), \\ F_{d(0)\to(3)}(x) = \dfrac{1}{2}\left(1 - \dfrac{L_x - x}{\sqrt{L_y^2 + (L_x - x)^2}} \right). \end{cases} \tag{9}$$

The expression of wall radiative entropy generation in terms of view factors is written as:

$$S_{g_{(0)}}(x) = \pi \int_{\nu=0}^{\nu=\infty} \begin{bmatrix} F_{d(0)\to(1)}(x)[S_\nu(I_{\nu\_ref}(x)) - S_\nu(I_\nu(T_{W_1}))] \\ + F_{d(0)\to(2)}(x)[S_\nu(I_{\nu\_ref}(x)) - S_\nu(I_\nu(T_{W_2}))] \\ + F_{d(0)\to(3)}(x)[S_\nu(I_{\nu\_ref}(x)) - S_\nu(I_\nu(T_{W_2}))] \end{bmatrix} d\nu, \quad (10)$$

where the reflected radiation intensity in the vertical direction is defined as:

$$I_{\nu\_ref}(x) = F_{d(0)\to(1)} I_\nu^b(T_{w_1}) + F_{d(0)\to(2)}(x) I_\nu^b(T_{w_2}) + F_{d(0)\to(3)}(x) I_\nu^b(T_{w_2}). \quad (11)$$

This last equation leads to:

$$I_{\nu\_ref}(x) = F_{d(0)\to(1)} I_\nu^b(T_{w_1}) + [1 - F_{d(0)\to(1)}(x)] I_\nu^b(T_{w_2}). \quad (12)$$

Using equation (12), the radiative entropy generation is given as follows:

$$S_{g_{(0)}}(x) = \pi \int_{\nu=0}^{\nu=\infty} S_\nu(I_{\nu\_ref}(x)) - F_{d(0)\to(1)}(x) S_\nu(I_\nu^b(T_{w_1})) - (F_{d(0)\to(2)}(x) + F_{d(0)\to(3)}(x)) S_\nu(I_\nu^b(T_{w_2})). \quad (13)$$

Equation (13) leads to:

$$S_{g_{(0)}}(x) = \pi \int_{\nu=0}^{\nu=\infty} S_\nu(I_{\nu\_ref}(x)) d\nu - \pi \cdot F_{d(0)\to(1)}(x) \cdot \int_{\nu=0}^{\nu=\infty} S_\nu(I_\nu^b(T_{w_1})) d\nu - \pi[1 - F_{d(0)\to(1)}(x)] \cdot \int_{\nu=0}^{\nu=\infty} S_\nu(I_\nu^b(T_{w_2})) d\nu. \quad (14)$$

By referring to Wu and Liu [24], this last equation can be written as follows:

$$S_{g(0)}(x) = \pi \int_{\nu=0}^{\nu=\infty} S_{\nu}(I_{\nu\_ref}(x))d\nu - \frac{4}{3}\sigma \cdot F_{d(0)\to(1)}(x)$$

$$\cdot T_{w_1}^3 - \frac{4}{3}\sigma \cdot [1 - F_{d(0)\to(1)}(x)] \cdot T_{w_2}^3. \quad (15)$$

Parallel to these calculations, we have proceeded to solve the problem through an approached model, reducing significantly the computation time. The basic idea of this approach is to suppose that the incident radiation originates locally from a unique fictitious black wall kept at a chosen reference temperature. Under such circumstances, the expression of the corresponding wall entropy generation becomes:

$$S_{g(0)}(x) = \frac{4}{3}\sigma \cdot F_{d(0)\to(1)}(x)[T_{ref}^3 - T_{w_1}^3]$$

$$+ \frac{4}{3}\sigma \cdot F_{d(0)\to(1)}(x)[T_{ref}^3 - T_{w_2}^3], \quad (16)$$

where T_{ref} represents the temperature of a unique surface, assuming the fact that radiation is issued from all walls. The corresponding expression of this chosen reference temperature is:

$$T_{ref}^4 = F_{d(0)\to(1)}(x)T_{w_1}^4 + [1 - F_{d(0)\to(1)}(x)]T_{w_2}^4. \quad (17)$$

Results and Discussion

Parallel plates

The first configuration already presented in Figure 1 illustrates the behaviour of thermal radiation from the black surface, reaching the perfectly reflective wall through the semi-transparent medium. A selection of figures is therefore elaborated to present the effect of the key parameters on radiative entropy production at the perfectly reflecting and diffuse wall.

Table 1. Quadrature effect (T_w = 1000K, T_a = 500 and $K.H$ = 1)

S_n	S_4	S_6	S_8	S_{10}	S_{12}
$S_g(\mathrm{W/K.m^2})$	0.7291	0.5169	0.4355	0.4038	0.3914
$q_{ri}(\mathrm{kW \cdot m^{-2}})$	15.0905	15.4255	15.4658	15.4504	15.4347

Even though the literature provides that the S_4 quadrature is sufficient to estimate radiative exchanges, we have proceeded to validate the choice of the quadrature through the calculation of both the radiative entropy creation at the reflective surface and incident radiative flux. When focusing on the figures of Table 1, the quadrature S_4 is not sufficient to have good precisions. Therefore, the consideration of the accuracy required, the S_{12} quadrature is chosen for all calculations reported in this study.

As we can see, Figure 4 and Figure 5, respectively, illustrate the effects of the ambient and the black surface wall temperatures on entropy generation. To put it another way, the entropy production is more developed when the difference between the black wall temperature and the ambient one is important. In addition, for a given temperature difference, the entropy generation is greater when the black wall temperature is higher than the ambient one. Moreover, the radiative entropy generation is attenuated increasingly when the black wall temperature approaches the ambient one.

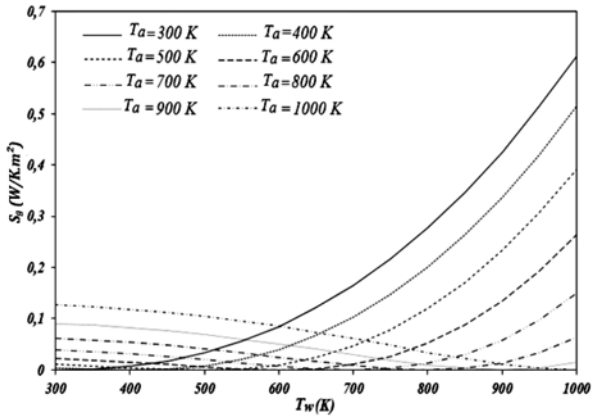

Figure 4. Effect of the ambient temperature on radiative entropy production with $K.H$ = 1.

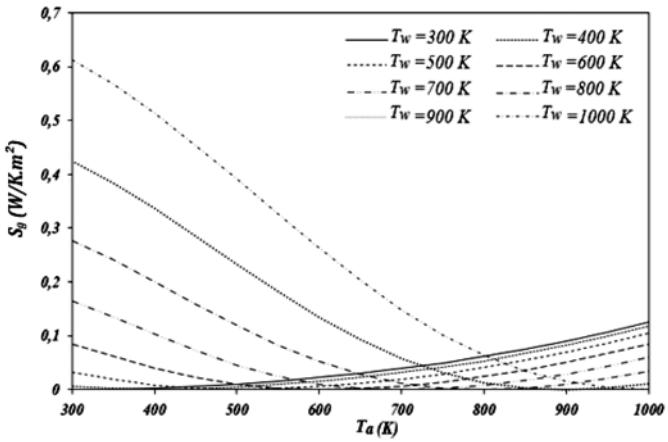

Figure 5. Effect of the black wall temperature on radiative entropy production with $K.H = 1$.

The variations of wall radiative entropy production which are represented in Figures 6 and 7, are given according to the optical thickness, for different ambient and black wall temperatures. At first blush, we can notice the existence of a relative maximum, which rises with the difference $|T_a - T_w|$, especially for higher ambient or black wall temperatures.

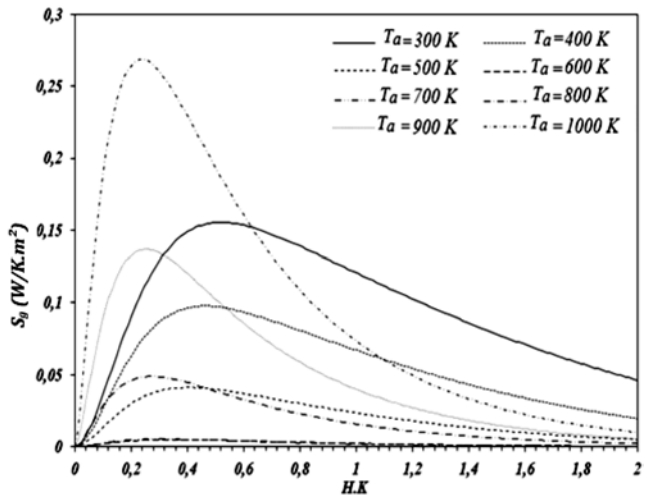

Figure 6. Variations of the entropy generation according to the optical thickness for different values of the ambient temperature, $T_w = 650$K.

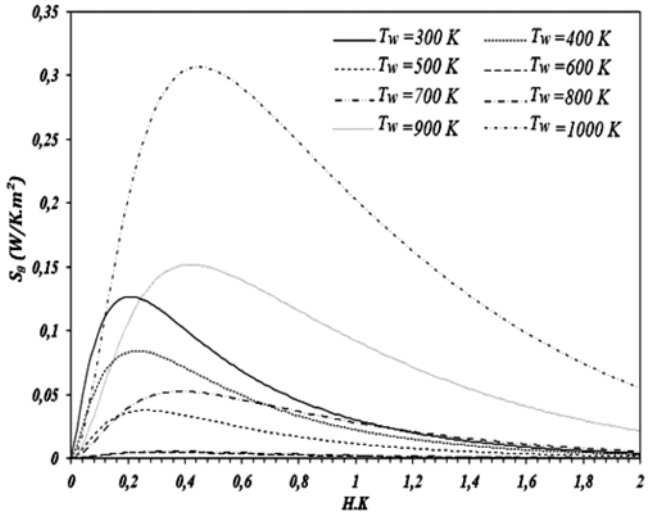

Figure 7. Variations of the entropy generation according to the optical thickness for different values of the black wall temperature; T_a = 650K.

It is worth noting that the optical thickness corresponding to the maximal entropy creation has been found to be independent of the chosen temperatures when the ambient temperature is higher than the black surface one. However, for an ambient temperature lower than the black surface one, the optical thickness corresponding to the maximal entropy generation augments when increasing the black surface temperature and diminishes when rising the ambient one. Furthermore, for lower optical thicknesses, the medium becomes transparent to radiation where the incident radiation is isotropic, arising from the same isothermal surface and explaining the remarkable decrease of entropy generated at the reflective surface. Similarly, for an optically thick medium, the incident radiation essentially due to gas emission at the uniform ambient temperature T_a is isotropic, explaining the asymptotic tendency towards zero of entropy creation for higher values of *K.H*.

Rectangular cavity

Figure 8 profiles the effect of the aspect ratio on wall radiative entropy production. In fact, for aspect ratios lower than the unit, the local entropy generation presents growing trends and concave profiles with a minimum value reached at the centre of the cavity and maximum values attained in vicinities of the side walls. In the opposite case, when the aspect ratio is equal or higher than the unit, entropy generation profiles are quasi uniform, exhibiting decreasing profiles with the aspect ratio.

Figure 9 illustrates the effect of aspect ratio on wall radiative entropy generation given for the same temperature difference $|T_{w1} - T_{w2}|$ used in Figure 8, but exchanging the corresponding wall temperatures. The results show a similarity between profiles of Figures 8 and 9 with the appearance of maxima in the vicinities of the side surfaces, in particular for low values of the aspect ratio. The virtue of the approach previously defined, is that satisfactory results are provided for aspect ratio lower than the unit in case of $T_{w1} > T_{w2}$ (Figure 8) and for aspect ratio higher than the unit when $T_{w1} < T_{w2}$ (Figure 9), respectively.

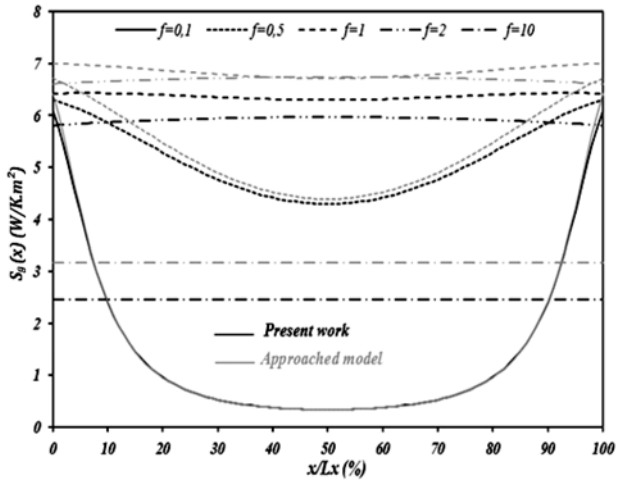

Figure 8. The effect of the aspect ratio on radiative entropy production, $T_{w1} = 1000\text{K}$, $T_{w2} = 300\text{K}$.

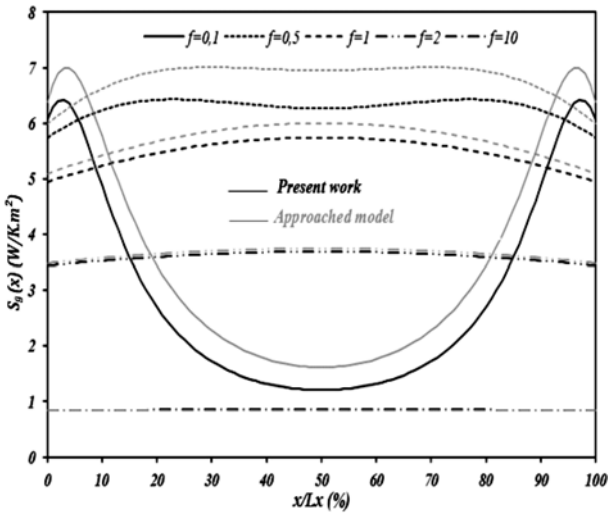

Figure 9. The effect of the aspect ratio on radiative entropy production, $Tw_1 = 300\text{K}$, $Tw_2 = 1000\text{K}$.

Figures 10 and 11 show, respectively, the effect of the upper and the lateral walls temperatures on the radiative entropy produced at the reflecting surface. As we can see in these diagrams, the entropy production clearly increases with the temperature difference $|T_{w1} - T_{w2}|$. What's more is that the profiles of entropy production become more developed when increasing separately the considered temperatures, presenting concave curves (Figure 10) when varying the upper wall temperature and slightly convex curves when varying the temperature of the side walls (Figure 11). Additionally, the results support the idea, that for a given vertical section and for a constant difference in the upper wall temperatures, the difference between the corresponding entropy creations is more important as well as raising T_{w1} (Figure 10). The same behavior takes place for a constant difference in the side walls temperatures as well as raising T_{w2} (Figure 11). A close look at Figure 10 clearly shows concavities with minima at the centre of the cavity. On the other hand, curves of Figure 11 display of three extrema with two maxima in vicinities of the side walls and a minimum located in the cavity centre, whereas the absolute minimum is located in close proximity to the side walls.

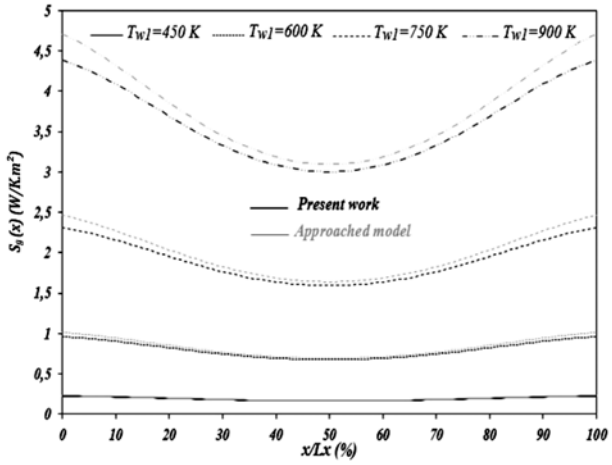

Figure 10. The effect of the upper wall temperature on radiative entropy production, $f = 0.5$, $T_{w2} = 300$K.

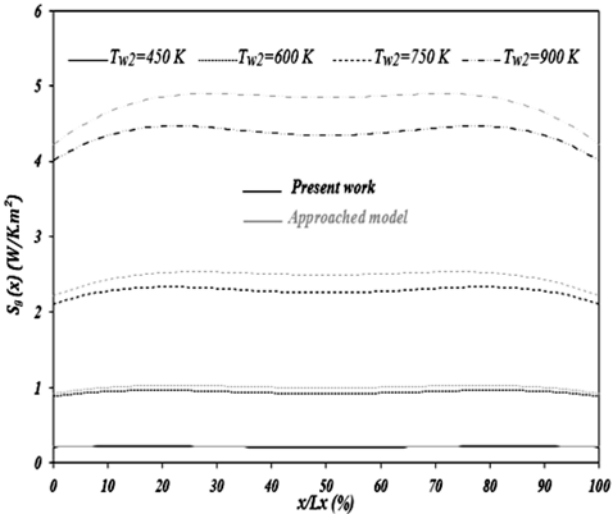

Figure 11. The effect of the side walls temperature on radiative entropy production, $f = 0.5$, $T_{w1} = 300$K.

In comparison to the results calculated using equation (16), it is reliable that raising the temperature difference $|T_{w1} - T_{w2}|$ increases the difference between entropy generation computed by our numerical model and by the approached one, respectively.

Conclusions

The analysis of radiative entropy generation at a perfectly reflecting and diffuse wall is investigated for two different cases. In the first one, we have considered a semi-transparent medium maintained between two parallel plates. In the second one, a non-participating medium is confined into a rectangular cavity with three black walls. In the light of what we have learned, we conclude:

- Case of parallel plates: even for low values of the optical thickness, the wall radiative entropy production increases with the difference between the ambient temperature and the black surface one.

- Case of rectangular cavity: according to the aspect ratio, the wall radiative entropy production increases for aspect ratio values lower than the unit and decreases for aspect ratio values higher than the unit.

Acknowledgement

The authors thank the anonymous referees for their valuable suggestions which led to the improvement of the manuscript.

References

[1] A. Agudelo and C. Cortés, Thermal radiation and the second law, Energy 35 (2010), 679-691.

[2] A. Bejan, A study of entropy generation in fundamental convective heat transfer, Journal of Heat Transfer 101 (1979), 718-725.

[3] A. Bejan, The thermodynamic design of heat and mass transfer processes and devices, International Journal of Heat and Fluid Flow 8 (1987), 258-276.

[4] F. Ben Nejma, A. Mazgar, N. Abdallah and K. Charrada, Entropy generation through combined non-grey gas radiation and forced convection between two parallel plates, Energy 33 (2008), 1169-1178.

[5] F. Ben Nejma, A. Mazgar and K. Charrada, Application of the statistical narrow band correlated-K model to entropy generation through non-grey gas radiation inside a spherical enclosure, International Journal of Exergy 8 (2011), 128-147.

[6] F. Ben Nejma, A. Mazgar and K. Charrada, Volumetric and wall non grey gas entropy creation in a cylindrical enclosure, WSEAS Transactions on Heat and Mass Transfer 5 (2010), 217-226.

[7] M. Caldas and V. Semiao, Entropy generation through radiative transfer in participating media: analysis and numerical computation, Journal of Quantitative Spectroscopy and Radiative Transfer 96 (2005), 423-437.

[8] M. Caldas and V. Semiao, The effect of turbulence-radiation interaction on radiative entropy generation and heat transfer, Journal of Quantitative Spectroscopy and Radiative Transfer 104 (2007), 12-23.

[9] S. X. Chu and L. H. Liu, Entropy generation analysis of two-dimensional high-temperature confined jet, International Journal of Thermal Sciences 48 (2009), 998-1006.

[10] S. Kabelac and R. Conrad, Entropy generation during the interaction of thermal radiation with a surface, Entropy 14 (2012), 717-735.

[11] W. Kröll, Properties of the entropy production due to radiative transfer, Journal of Quantitative Spectroscopy and Radiative Transfer 7 (1967), 715-723.

[12] L. H. Liu and S. X. Chu, On the entropy generation formula of radiation heat transfer processes, Journal of Heat Transfer 128 (2006), 504-506.

[13] L. H. Liu and S. X. Chu, Radiative energy transfer equation, Journal of Thermophysics and Heat Transfer 21 (2007), 819-822.

[14] L. H. Liu and S. X. Chu, Verification of numerical simulation method for entropy generation of radiative heat transfer in semitransparent medium, Journal of Quantitative Spectroscopy and Radiative Transfer 103 (2007), 43-56.

[15] A. Mazgar, F. Ben Nejma and K. Charrada, Entropy generation through combined non-grey gas radiation and natural convection in vertical pipe, Progress in Computational Fluid Dynamics 9 (2009), 495-506.

[16] A. Mazgar, F. Ben Nejma and K. Charrada, Second law analysis of coupled mixed convection and non-grey gas radiation within a cylindrical annulus, International Journal of Mathematical Models and Methods in Applied Sciences 7 (2013), 265-276.

[17] J. Oxenius, Radiative transfer and irreversibility, Journal of Quantitative Spectroscopy and Radiative Transfer 6 (1966), 65-91.

[18] M. Planck, The Theory of Heat Radiation, Dover, New York, 1959.

[19] M. Planck, Theorie der Wärmestrahlung, 2. Aufl. I. A. Barth, Leipzig, 1913.

[20] J. Y. San, W. M. Worek and Z. Lavan, Entropy generation in combined heat and mass transfer, International Journal of Heat and Mass Transfer 30 (1987), 1359-1369.

[21] J. Y. San, W. M. Worek and Z. Lavan, Entropy generation in convective heat transfer and isothermal convective mass transfer, Journal of Heat Transfer 109 (1987), 647-652.

[22] R. Wildt, Radiative transfer and thermodynamics, The Astrophysical Journal 123 (1956), 107-116.

[23] S. E. Wright, D. S. Scott, J. B. Haddow and M. A. Rosen, On the entropy of radiative heat transfer in engineering thermodynamics, International Journal of Engineering Science 39 (2001), 1691-1706.

[24] W. Wu and Y. Liu, Radiation entropy flux and entropy production of the earth system, Reviews of Geophysics 48 (2010), 1-27.

[25] Z. M. Zhang and S. Basu, Entropy flow and generation in radiative transfer between surfaces, International Journal of Heat and Mass Transfer 50 (2007), 702-712.